Extension of Electron Dissipation Region along the Downstream Direction in Steady Collisionless Driven Reconnection

Bin Li, Ritoku Horiuchi[1,2)]

The Graduate University for Advanced Studies,322-6 Oroshi-cho, Toki 509-5292, Japan
[1)] *The Graduate University for Advanced Studies,322-6 Oroshi-cho, Toki 509-5292, Japan*
[2)] *Department of Simulation Science, National Institute for Fusion Science, 322-6 Oroshi-cho, Toki 509-5292, Japan*

(Received: 26 August 2008 / Accepted: 9 December 2008)

Steady collisionless driven reconnection in an open system is investigated by means of 3D full-particle simulations. When the system relaxes to the steady state, a long and narrow current sheet and electron dissipation region are formed in the downstream direction. The Sweet-Parker model predicts that outflow peak will appear at the edge of electron dissipation region. However, the electron dissipation region still extends far away from the peak position toward the downstream direction, which is due to the strong electron outflow. The reason why such a two-scale structure is maintained in the steady state is investigated from a viewpoint of energy conversion. It is found that the dissipated magnetic energy is converted firstly to electron kinetic energy in the driving electric field direction at the reconnection point, and then most of this energy is converted to electron outflow kinetic energy during electrons move towards the edge of the inner structure of the electron dissipation region in the downstream direction.

Keywords: steady driven reconnection, electron dissipation region, energy conversion

1. Introduction

Magnetic reconnection refers to breaking frozen-in magnetic flux and reconnecting reversed field lines. It is one of most important dynamic phenomena in magnetized plasmas and its mechanism has been focus on over half-century [1]. Through magnetic reconnection magnetic energy is converted to plasma kinetic and thermal energy.

The reconnection takes place in the dissipation region, the structure of which has been investigated since the establishment of two well-known models, namely, Sweet-Parker model [2, 3] and Petschek model [4], which are in the framework of resistive magneto-hydrodynamics(MHD). Sweet-Parker model [2, 3] assumes resistive diffusion process as a cause of magnetic energy dissipation. However, the time scale of magnetic energy release in solar flares predicted by Sweet-Parker model is much longer than the observation value. This slowness is due to the fact that model assuming both plasma outflow and magnetic flux have to go through a long and narrow neutral sheet, which is a natural result of small resistivity calculated from classical Spitzer resistivity [5].

In Petschek model [4] outflow region away from the X-shaped separatrix is regarded as an expansion fan [4, 1], which introduces a smaller dissipation region and thus reconnection rate is much faster. Some researchers have demonstrated that Petschek geometry can not be achieved if a spatially uniform resistivity exists [6, 7, 8] but it can be reduced to Sweet-Parker model under such certain conditions [7, 8]. Thus Petschek model may be considered as a special case of the Sweet-Parker model in this sense.

On the other hand, analyses of Magnetic Reconnection Experiment (MRX) [9] and Wind satellite observations [10] suggested that current sheet generated in the reconnection has a similar spatial configuration as that Sweet-Parker model predicted, while the dissipation mechanism is different from the classical resistivity. In general this result is considered to be expected from microscale particle kinetic effects, i.e., the inertia effect[11, 12, 13] or the thermal effect [11, 14, 15, 16] based on the non-gyrotropic meandering motion, which have proved by a serials of two dimensional simulations [12, 13, 14, 15, 16, 17, 18].

Recent numerical simulation [19, 20] has indicated that electron dissipation region (EDR) forms a long narrow layer in downstream direction and has a multi-scale structure in nonlinear evolution stage, while reconnection rate still remains fast. The elongation of the EDR is attributed to the strong outward convection of magnetic flux [20]. While in this letter, we show that prolongation of EDR is deeply related to the spatial profile of electron outflow speed in downstream direction in the steady state and explain how its spatial profile is developed in the steady driven reconnection from a viewpoint of the energy conversion.

The steady driven reconnection is investigated by three dimensional particle-in-cell (PIC) code

author's e-mail: li.bin@nifs.ac.jp

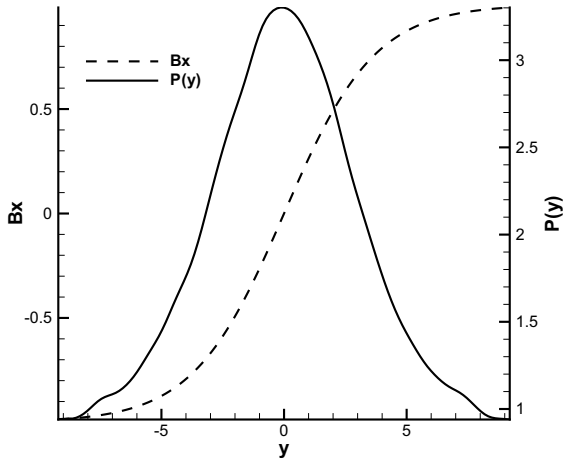

Fig. 1 Profiles of magnetic field $B_x(y)$ and plasma pressure $P(y)$ in initial Harris current sheet. These two quantities have no variations in x (downstream)direction.

"PASMO" [17, 18, 21, 22, 23], which 2D version already has been used in previous investigations [14, 15, 17, 18].

Two 3D simulation runs were adopted in the current research. In both cases, the simulation domain is implemented on a $258 \times 129 \times 66$ point grid corresponding to size $(73.85 \times 18.5 \times 14)\,(c/\omega_{ce})^3$ and 2.11×10^8 particles are used. The initial time step is $\Delta t\omega_{ce} = 0.072$ and electron skin depth is $d_e \approx 3.4\lambda_{de}$. As an initial condition we employ an one-dimensional Harris equilibrium with magnetic field and plasma pressure as $B_x(y) = B_0 \cdot \tanh(y/y_h)$, $P(y) = B_0^2/8\pi \cdot \mathrm{sech}^2(y/y_h)$, with the scale height y_h, which is shown in Fig. 1. The ratio of electron Larmor radius to the scale height is $R_e/y_h = 0.078$. The distribution of particles is a shifted Maxwellian with a uniform temperature $\mathrm{T_{i0}} = \mathrm{T_{e0}}$. We set the ratio of ion to electron masses $\mathrm{m_i/m_e} = 100$, that of electron plasma frequency to the electron cyclotron frequency $\omega_{\mathrm{pe0}}/\omega_{\mathrm{ce0}} = 2$, and the ratio of input window size of driving electric field to inflow direction length $\mathrm{x_d} = 1.5$ in numerical simulations[17].

It is assumed that the boundary condition at $z = \pm z_b$ along z axis are periodic, and physical quantities are integrated along the z direction to produce figures shown in this paper. Plasma inflow is driven into the simulation domain by driving electric field imposed at the upstream boundary at $y = \pm y_b$. The driving electric field is finite only within the input window size x_d around $x = 0$ during the Alfvén time $\tau_A = \mathrm{y_b/V_A}$, where $\mathrm{V_A}$ is the initial average Alfvén velocity. After that the strength of the driving electric field becomes uniform at the upstream boundary.

Plasma outflow goes through simulation domain through the downstream boundary at $x = \pm x_b$, where field quantities $\partial_x E_y$, $\partial_x E_z$ are continuous, and $\partial_x E_x$ is zero at the downstream boundary, which enable magnetic islands go through the boundary. The other components of the electromagnetic field can be obtained by solving Maxwell equations at the downstream boundary [17, 18, 21, 22, 23].

Because we are interested in the cause of the extension of EDR in the driven reconnection from a viewpoint of the energy conversion, we change parameters related to the energy input from the external energy source, as a result, which will influence the energy conversion process of the driven reconnection. In our driven reconnection model, the energy input is mainly controlled by the strength of the driving electric field, which can be expressed by the strength of the inflow velocity $\mathrm{E_0/B_0}$. In this paper we performed two simulation runs: run1 and run2 corresponding to $\mathrm{E_0/B_0} = -0.04\mathrm{c}$, and $\mathrm{E_0/B_0} = -0.02\mathrm{c}$, respectively.

2. Simulation Result

With the driving electric field and prescribed magnetic field B_x, plasma is driven into the simulation domain by performing $E \times B$ drift motion. Meanwhile magnetic field lines also bend toward the center of simulation domain. It causes both plasma density and gradient of magnetic field B_x to increase at the center along inflow direction. Then magnetic reconnection takes place at the center, and the X-shaped separatrix is formed there too.

When the value of electric field E_z at the reconnection point equals the value of driving electric field E_z imposed at the upstream boundary, the system relaxes to the steady state. A long and narrow current sheet is formed along the downstream direction in the steady state [24], which is a typical feature of Sweet-Parker model's prediction. The width of current sheet is in the scale of electron skin depth and meandering scale [24], and thus the width of electron dissipation region and current sheet are in the same scale too.

On the other hand, it is found that in both cases the EDR has a two-scale structure along the downstream direction. Its shape is a rectangular nested within a much longer rectangular inside the plane perpendicular to the driving electric field. Furthermore weakening the strength of the driving electric field in the run2 does not change the two-scale structure in the steady state of run2.

Contour plots of the EDR of two simulation runs in the steady state are shown in Fig. 2, in which a two-scale structure is presented in the downstream direction, the inner structure and outer structure of which are indicated in blue and red, respectively. The contour legend of Fig. 2 stands for the physical quantity

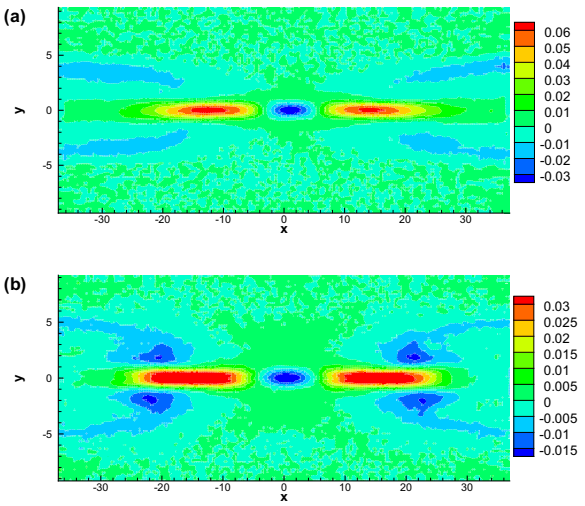

Fig. 2 Contour plots of the electron dissipation region in the (x, y) plane in the steady state where figures are plotted after being averaged from $t\omega_{ce} = 1301$ to $t\omega_{ce} = 1593$. The label (a) and (b) corresponds to the case of run1 and run2, respectively. The color in figures indicates the value of the term $(E+v_e\times B)_z$.

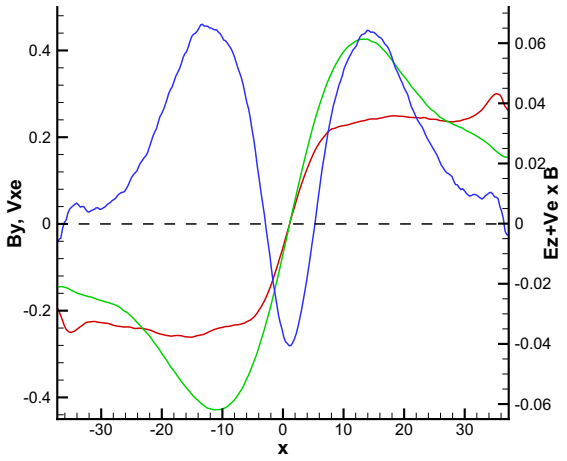

Fig. 3 Spatial profiles of physical quantities passing through the reconnection point in downstream direction in the steady state for the same case as Fig. 2(a) in simulation run1, where electron outflow velocity v_{xe}, reconnected magnetic field B_y, and quantity $(E + v_e \times B)_z$ are indicated in green, red, and blue, respectively.

$(E + v_e \times B)$, the value of which are negative and positive in blue region and red region, respectively. The variance oh the EDR in color indicates that different physical mechanism accounts for the breaking of the magnetic field lines there.

The appearance of different contour legends in Fig. 2 indicates that the peak value of $(E + v_e \times B)_z$ of two runs are different. Because the value of electric field E_z is constant and similarity in structures of EDR between two cases in the steady state, it implies that patterns of spatial profiles of electron outflow v_{xe} and magnetic field B_y are similar between two cases in spite of their peak values are different in the steady state, which is confirmed by our comparison between two runs. The following discussions on the features of structure of EDR are mainly based on results of run1.

The inner region of EDR is stretched away from the reconnection point, around where the magnitude of the cross product of electron bulk velocity and magnetic fields is smaller than that of electric field E_z. Therefore electrons satisfy $(E + v_e \times B)_z < 0$ inside the inner region of EDR, as indicated in blue in Fig. 2.

Away from the edge of the inner structure, the cross product of electron bulk velocity and magnetic fields increases continually along downstream direction, and is larger than that of electric field E_z there. As a result, electrons satisfy $(E + v_e \times B)_z > 0$ inside the outer region of EDR, as indicated in red in Fig. 2.

Next, let us consider spatial variation of the quantity $(E + v_e \times B)_z$ in downstream direction in a more detail. It is easy to know that the spatial variation of the quantity $(E + v_e \times B)_z$ mainly depends on that of the electron outflow speed v_{xe} and reconnected magnetic field B_y in outflow direction, while electric field E_z is constant throughout simulation domain in the steady state. Spatial profiles of electron outflow speed v_{xe}, reconnected magnetic field B_y, and quantity $(E + v_e \times B)_z$ passing through the reconnection point in downstream direction in simulation run1 are compared in Fig. 3 to assist the analysis.

It can be seen in Fig. 3 that $(E + v_e \times B)_z \approx 0$ around $|x| \approx 6$, and the reconnected magnetic field B_y becomes flat there. It is expected that if electron outflow keeps its value for $|x| > 6$, electron frozen-in region will be extended further in downstream direction. However, electron outflow speed continues to increase until it reaches its maximum value around $|x| \approx 12$, and the outer region of EDR is formed as a consequence.

Because the magnitude of the term $v_e \times B$ increases with the distance away from the reconnection point due to strong electron outflow, the quantity $(E + v_e \times B)_z$ changes its sign from negative to positive in downstream direction. In this sense, it is easy to infer that the EDR do have a two-scale structure, and the outer structure of EDR will be extended more longer in downstream direction in case of strong electron outflow.

The classical Sweet-Parker model implies that the edge of EDR is located at a place where electron outflow speed maximizes. In the simulation, however, this place appears only as a boundary between two dis-

tinct regions of EDR, which is due to the strong electron outflow as discussed above. Thus, the question how EDR is extended and forms a two-scale structure is equivalent to the question how strong electron flow is generated in the steady state as shown in Fig. 3. It is believed that strong electron outflow is produced by Lorentz force in the nonlinear evolution stage, and keeps its spatial shape in the steady state. An energy conversion process is necessary to maintain strong electron outflow in the steady state, namely, the energy should be converted to electron outflow kinetic energy.

Figure 4 shows spatial profiles of electron kinetic energies along the downstream direction passing through the reconnection point in the steady state. The electron kinetic energy in the outflow direction starts to grow from the reconnection point and maximizes around $|x| \approx 12$. On the other hand, the electron kinetic energy in the z direction reduces its maximum value from the reconnection point until the electron outflow energy reaches its peak value.

The evolutions of the two electron energies indicates that electron kinetic energy is conserved along the downstream direction, i.e., the sum of them is nearly a constant until the electron outflow energy maximizes, as shown in Fig. 4. In other words, the electron kinetic energy in the z direction is converted to the electron kinetic energy in the downstream direction ranging from the the reconnection point to the place where electron outflow speed reaches its peak value. This process actually is mediated by Lorentz forces because they do not lead to the change in the total energy, which is shown in a recent investigation [25].

In the previous investigation[26], we have clarified the relationship between the magnetic energy density at the edge of EDR in the inflow direction and maximum electron outflow kinetic energy density in downstream direction based on the same simulation as

$$\frac{1}{2} m_e n_e v_{e,out}^2 = \frac{B_{x,in}^2}{8\pi}, \tag{1}$$

where LHS is the peak value of the outflow electron kinetic energy density at the edge of the inner structure of the EDR in the outflow direction, and RHS stands for the magnetic energy density carried into EDR in the inflow direction.

Now it can be concluded that the magnetic energy is initially converted electron kinetic energy in z direction, and then it converted to electron kinetic energy in outflow direction at the edge of inner structure of the EDR.

3. Summary

When the system relaxes to the steady state, the reconnection electric field equals driving electric field

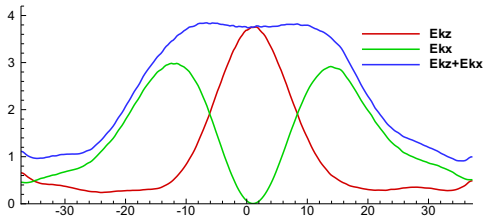

Fig. 4 Spatial profiles of electron kinetic energies passing through the reconnection point in downstream direction in the steady state for the same case as Fig. 2(a) in simulation run1, where electron kinetic energy in z direction, electron kinetic energy in downstream direction, and the sum of the two direction kinetic energies are indicated in red, green, and blue, respectively.

imposed at the upstream boundary. Meanwhile EDR has two distinct structures in the downstream direction in spite of variation of strength of external energy input, which are deeply related to the existence of strong electron outflow.

To maintain the strong electron outflow in the steady state, an energy conversion process is required from the viewpoint of energy conversion. The energy converted to electron outflow kinetic energy comes from the dissipated magnetic energy carried by electrons flow into the EDR in inflow direction. The process has two steps. First, the dissipated magnetic energy is converted to electron kinetic energy in the z direction at the reconnection point. Second, most of the electron kinetic energy in the z direction is converted to the electron kinetic energy in the downstream direction in the range from the reconnection point to the edge of inner structure of EDR, around which electron outflow speed maximizes.

This work was partially supported by a Grant-in-Aid for Scientific Research from Japan Society for the Promotion of Science (No. 18340188), the Research Cooperation Program on "Hierarchy and Holism in Natural Sciences 2" at National Institutes of Natural Sciences, and General Coordinated Research at National Institute for Fusion Science (NIFS08KTAN005).

[1] D. Biskamp. *Magnetic Reconnection in Plasmas.* Cambridge University Press,Cambridge, 2000.
[2] P. A. Sweet. *in Electromagnetic Phenomena in Ionized Gases.* 1958.
[3] E. N. Parker. *Astrophys.J.,Suppl.*, 8:177, 1963.
[4] H. E. Petschek. *in AAS-NASA Symposium on Solar Flares NASA SP50.* 1964.
[5] Lyman Spitzer and Richard Härm. Transport phenomena in a completely ionized gas. *Phys. Rev.*, 89(5):977–981, Mar 1953.
[6] D. Biskamp. *Phys. Fluids.*, 29:1520, 1986.
[7] Russell M. Kulsrud. *Earth Planets Space*, 53:417,

2001.
[8] Leonid M. Malyshkin, Timur Linde, and Russell M. Kulsrud. *Phys. Plasmas.*, 12:102902, 2005.
[9] Hantao Ji, Masaaki Yamada, Scott Hsu, and Russell Kulsrud. *Phys. Rev. Lett.*, 80:3256, 1998.
[10] M. Oieroset, T. D. Phan, M. Fujimoto, R. P. Lin, and R. P. Lepping. *Nature*, 414:412, 2001.
[11] V. M. Vasyliunas. *Rev. Geophys.*, 13:303, 1975.
[12] M. Ottaviani and F. Porcelli. *Phys. Rev. Lett.*, 71:3802, 1993.
[13] D. Biskamp, E. Schwarz, and J. F. Drake. *Phys. Rev. Lett.*, 75:3850, 1995.
[14] R. Horiuchi and T. Sato. *Phys. Plasmas.*, 1:3587, 1994.
[15] R. Horiuchi and T. Sato. *Phys. Plasmas.*, 4:277, 1997.
[16] IM. Hesse, K. Schindler, J. Bim, and M. Kuznetsova. *Phys. Plasmas.*, 6:1781, 1999.
[17] W. Pei, R. Horiuchi, and T. Sato. *Phys. Plasmas.*, 8:3251, 2001.
[18] A. Ishizawa, R. Horiuchi, and H. Ohtani. *Phys. Plasmas.*, 11:3579, 2004.
[19] MA Shay, JF Drake, and M. Swisdak. *Physical Review Letters*, 99(15):155002, 2007.
[20] H. Karimabadi, W. Daughton, and J. Scudder. *Geophysical Research Letters*, 34(13), 2007.
[21] R. Horiuchi, H. Ohtani, and A. Ishizawa. *J. plasma phys.*, 72:953, 2006.
[22] H. Ohtani, S. Ishiguro, R. Horiuchi, Y. Hayashi, and N. Horiuchi. *Lecture Notes of Computer Science in press*, 94:262, 2007.
[23] H. Ohtani, R. Horiuchi, and A. Ishizawa. *J. plasma phys.*, 72:929, 2006.
[24] Bin Li, Ritoku Horiuchi, and Hiroaki Ohtani. *Plasma Fusion Res.*, 3:S1054, 2008.
[25] Bin Li, R. Horiuchi, and H. Ohtani. *Annual report of National Institute of Fusion Science, 2007,to be published.*
[26] Bin Li, R. Horiuchi, and H. Ohtani. *Annual report of National Institute of Fusion Science*, 5(21):356, 2006.